sustainability

MDPI

Article

Modeling and Mapping of Soil Salinity and its Impact on Paddy Lands in Jaffna Peninsula, Sri Lanka

Tharani Gopalakrishnan * and Lalit Kumar

School of Environmental and Rural Science, University of New England, Armidale 2351, Australia; lkumar@une.edu.au

* Correspondence: tgopalak@myune.edu.au

Received: 23 September 2020; Accepted: 6 October 2020; Published: 9 October 2020

Abstract: Soil salinity is a major threat to land productivity, water resources and agriculture in coastal areas and arid and semi-arid regions of the world. This has a significantly negative effect on the land and causes desertification. Monitoring salt accumulation in the soil is crucial for the prevention of land degradation in such environments. This study attempted to estimate and map soil salinity in Jaffna Peninsula, a semi-arid region of Sri Lanka. A Partial Least Squares Regression (PLSR) model was constructed using Sentinel 2A satellite imagery and field-measured soil electrical conductivity (EC) values. The results showed that satisfactory prediction of the soil salinity could be made based on the PLSR model coupled with Sentinel 2A satellite imagery (R^2 = 0.69, RMSE = 0.4830). Overall, 32.8% of the land and 45% of paddy lands in Jaffna Peninsula are affected by salt. The findings of this study indicate that PLSR is suitable for the soil salinity mapping, especially in semi-arid regions like Jaffna Peninsula. The results underpin the importance of building adaptive capacity and implementing suitable preventive strategies for sustainable land and agricultural management.

Keywords: soil salinity; Jaffna Peninsula; Sentinel 2; remote sensing; salinity indices; soil mapping; paddy lands; sustainability

1. Introduction

Soil salinization is one of the world's most significant environmental soil hazards, which results in severe land degradation and desertification. This is caused by both natural and anthropogenic activities [1,2]. The excess accumulation of soluble salts in the soil surface is referred to as salinization, which has an adverse impact on agricultural production, biodiversity and sustainable development. Saline soils predominantly occur in arid and semi-arid regions, where evapotranspiration exceeds rainfall, as well as in coastal regions as a result of seawater intrusion and coastal tidal inundation.

In recent years, many national and international policies have focused on soil protection against soil threats [3,4]. There are more than 800 million hectares of land globally affected by salinity [5], and this extent is expected to increase in the future [6]. It is estimated that 20% of total cultivated and 33% of irrigated agricultural areas in the world have been affected by high salinity, and by 2050, more than 50% of arable lands are expected to be salinized [7]. High concentrations of salt in agricultural soil or irrigation water affect almost all stages of the crop life cycle: from germination, to the uptake of water and necessary nutrients, thereby reducing plant growth and significantly reducing crop yields. Soil salinity also imposes ion toxicity, osmotic fragility and oxidative stress on crops, thereby limiting the water absorption [8].

The regular monitoring of soil salinity for accurate information about its spatial extent and magnitude of severity is essential for efficient land and water management in affected agricultural areas. This can be achieved through mapping the electrical conductivity (EC) of the soil [9]. However, conventional methods of field-based surveys are expensive and time-consuming. A large number

of samples are required to adequately characterize salinization over broad areas as soil salinity shows high spatial variability over short distances. Remote sensing has been recognized as a promising technique for detecting and mapping soil salinity over the recent decades [10]. The relationship of spectral information extracted from the satellite data with soil reflectance spectra provides the ability to monitor and map regional and global soil salinity with greater efficiency and at low cost in a shorter period of time [11].

Spectral indices derived from satellite images have proven to be important in soil salinity mapping [12]. Multispectral satellite imageries, in particular Landsat series, have been widely used to produce EC maps, and they are available at no cost, however their accuracy is often limited by the coarse resolution (30 m multispectral resolution). The new generation Sentinel 2A satellite, equipped with a Multi-Spectral Instrument (MSI), launched in 2015, offers freely available optical imageries with high spatial (up to 10 m) and spectral resolution (13 spectral bands), and with short revisit cycles (5 days). Recent studies have highlighted the great potential of this Sentinel 2A satellite imagery for soil salinity mapping [13–16], compared to Landsat 8 OLI [17–20].

Soil salinity is an enormous problem in coastal regions and the irrigated lands in dry zones of Sri Lanka. Approximately 11,200 ha of coastal lands have been affected and more than 50% of the coastal paddy lands have been abandoned due to salinity [21]. Jaffna Peninsula, located in the northern most part of Sri Lanka, is one of the most salt-affected regions in Sri Lanka. Salinity has been a devastating threat to the fresh water and coastal lowlands of the region. Geographically, the relatively flat terrain of the Jaffna Peninsula enhances the vulnerability to intrusion of seawater. The total elevation ranges from –1.9 masl to 15 masl, and more than 89% of the land is below 5 masl. Moreover, as a semi-arid region, high evaporation rates along with short-term precipitation induces top soil salinization. Furthermore, the majority of the population depends on groundwater for their daily needs and livelihood, as there are no perennial rivers or major water supply systems in the region. Therefore, extensive usage of groundwater greatly exacerbates the salt migration into groundwater and further inland [22,23]. Evidence of groundwater salinization along the coastal areas around the lagoons is well reported. Previous studies have reported that a significant number of wells and hundreds of acres of land have been abandoned due to salinity [24–26]. In a study by Gopalakrishnan, et al. [27], it was established that during the last three decades, 8178 ha of paddy lands were permanently abandoned and groundwater salinity increased 1.6-fold.

However, there is no published information related to soil salinity in the Jaffna Peninsula region. To date, there has been no attempts to investigate the extent, magnitude and severity of soil salinity in the Peninsula. Thus, to fill this gap, this study aims to examine the current status of soil salinization in Jaffna Peninsula. The specific objectives of this study were to (1) estimate and map the spatial variation of soil salinity in Jaffna Peninsula using remote sensing and GIS techniques, (2) explore the potential of Sentinel 2A satellite data to map the soil salinity over the semi-arid landscape of Jaffna Peninsula, and (3) assess the extent and magnitude of soil salinity over the paddy lands of Jaffna Peninsula. To the best of our knowledge, this is the first study to map the salinity in Jaffna Peninsula over a large area using remote sensing techniques. This information is of critical importance for farmers, land use planners, policy makers and stakeholders in developing effective soil restoration and sustainable management strategies for the salt-affected lands. It should also be noted that extensive ground surveys in Jaffna Peninsula are fraught with danger due to unexploded ordinances left behind by the civil war, hence a remote sensing-based solution would be extremely useful for the mapping and long term monitoring of soil salinity.

2. Materials and Methods

2.1. Study Area

Jaffna Peninsula is located in the northern most part of Sri Lanka, between longitude 79°38′4′′ E to 80°34′56′′ and latitude 9°49′17′′ to 9°28′13′′ N, and occupies an area of about 1050 sq km (Figure 1).

The topography is relatively flat, with median elevation of 2 masl. Jaffna Peninsula falls into a low country dry zone with annual precipitation of 1290 mm and an average annual temperature of 29.5 °C. More than 90% of the rainfall is received during the four months from October to January. The period between two monsoon seasons is dry and extends from June to September. The entire Jaffna Peninsula is predominantly underlined by Miocene limestone, which is compact, indistinctly bedded and highly karstified [28]. The major soils are calcic red yellow latosols in the central region where high-value arable crops are cultivated. In addition, alkaline and saline rega soils are dominant in the coastal areas where paddy crops are cultivated. Jaffna Peninsula is predominantly an agricultural area, however the rapidly increasing salinity in agricultural lands has been adversely impacting the livelihoods of the people residing in the region.

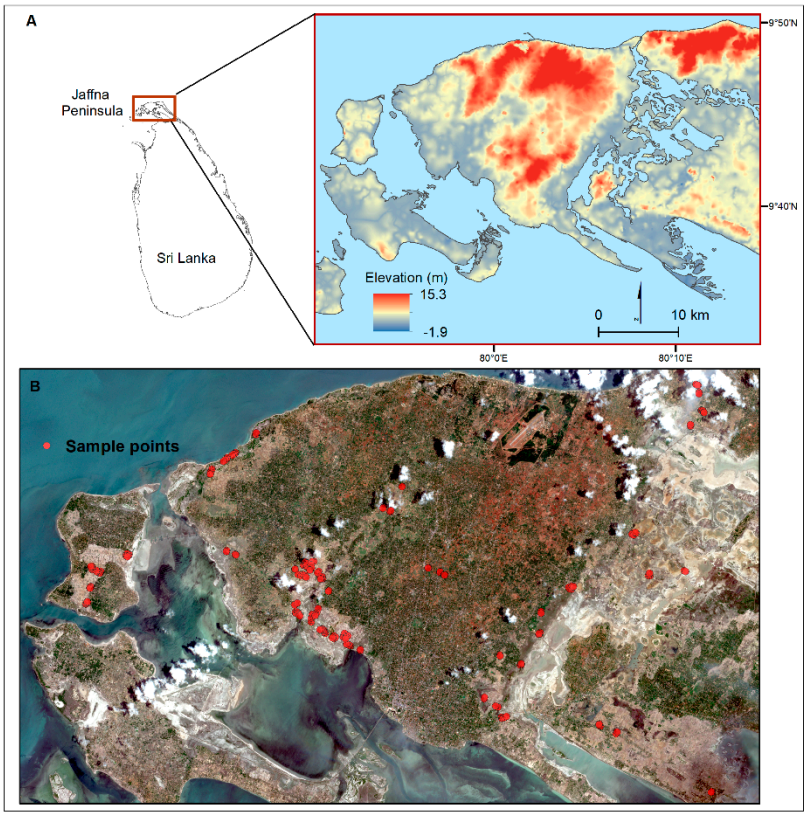

Figure 1. Location of the study area (**A**). Location of Jaffna Peninsula in northern Sri Lanka with a Digital Elevation Model (DEM) (**B**). Sampling locations on a true color composite of Sentinel 2A satellite imagery, 2019.

2.2. Soil Sample Collection and Laboratory Analysis

Soil sample location sites were selected based on the amounts of vegetation and agricultural land use classes. A field survey was conducted during August 2019, which is the peak of the dry season and the fallow season of paddy cultivation for Jaffna Peninsula. A total of 198 soil samples were collected using hand augers at a constant depth of 15–20 cm (Figure 1). At each sampling point, four sub samples were collected at a distance of 1 m north, south, east and west of the center of the core sampling point. The sub samples were then thoroughly mixed in the field to make one representative composite sample from the five sub-samples collected. The coordinates of each sample were recorded using a portable Global Positioning System (GPS) Garmin Montana 680t (accuracy ≤ 3 m).

Soil samples were then sealed, labelled and transferred to the lab for analysis. The soil samples were air-dried at normal temperature in the lab, manually ground and sieved using a 2 mm sieve to remove gravel and foreign matter. The samples were analyzed for determining salinity using 1:5 soil

saturation extract method [9]. To prepare the soil suspensions, 100 mL of distilled water was added to each 20 g of soil sample. These suspensions were then continuously shaken by using a mechanical shaker for 60 min in order to dissolve the soluble salts. After mixing, the saturation extracts were kept to settle for 30 min and EC was measured using an electrical conductivity meter at 25 °C.

2.3. Satellite Image Acquisition and Processing

The remote sensing data used in this study were from Sentinel 2A, which is a polar orbiting satellite mission of the European Copernicus Program. The Sentinel 2A satellite carries a Multi-Spectral Instrument (MSI) on board and acquires optical images at high resolutions. It provides multispectral data with 13 bands, spanning through visible, near infrared (NIR) and shortwave infrared (SWIR) at different spatial resolutions ranging from 10 m to 60 m (Table 1). The Sentinel 2A Level-1C (L1C) MSI data of 8 September 2019 with cloud cover less than 11% were downloaded from Sentinel's Scientific Data Hub (https://scihub.copernicus.eu/). This was the best possible image of Jaffna Peninsula during the study period that had the least cloud cover. L1C datasets have geometric- and radiometric-corrected top of atmosphere reflectance. Atmospheric correction of the image was performed using the Sen2cor plugin v 02.08.00 available on the Sentinel Application Platform (SNAP) toolbox version 7.0 where the top of atmosphere (TOA) reflectance values were converted to bottom of atmosphere (BOA) reflectance values. The image was then projected in WGS 1984 UTM zone 44 N and subset/clipped to the study area.

Table 1. Characteristics of the Multi-Spectral Instrument (MSI) on board the Sentinel 2A satellite.

Bands	Band Center (nm)	Band Width (nm)	Spatial Resolution (m)
Coastal aerosol	433	20	60
Blue	490	65	10
Green	560	35	10
Red	665	30	10
Vegetation Red Edge (Red Ed1)	705	15	20
Vegetation Red Edge (Red Ed 2)	740	15	20
Vegetation Red Edge (Red Ed 3)	783	20	20
Near Infra-Red NIR	842	115	10
NIR narrow (NIRn)	865	20	20
Water Vapour	945	20	60
Cirrus	1380	30	60
Short Wave Infrared (SWIR1)	1610	90	20
Short Wave Infrared (SWIR2)	2190	180	20

2.4. Selection of the Optimal Spectral Index for Estimating Soil Salinity

In total, 14 soil salinity indices were developed from the Sentinel 2A satellite image based on their potential for salt detection (Table 2). Logarithmic transformation was applied to the EC data as it provides better accuracy. Soil samples that fell in the cloud cover patches of the satellite image were excluded. The whole dataset (n = 184) was divided into two sets; a calibration set of 147 soil samples (80% of the whole soil samples) and a validation set of 37 soil samples (20% of the whole soil samples) for cross validation, respectively. PLSR was employed to model the relationship between EC and spectral indices. Other regression models such as multiple linear regression and support vector regression were also examined, but did not provide adequate accuracy, hence only the PLSR model is explained here. PLSR is a bilinear regression technique that combines features from principal component analysis and multiple regression. It offers greater predictive power when predictor variables exhibit multiple collinearity. This is achieved by extracting a set of eigenvectors called latent variables from the independent/predictor data matrix which have the best predictive power. Pearson correlation

co-efficient R (PCC) and variable importance (VIP) were used to choose the appropriate/ best variables for the models. Full cross validation was applied to select the optimum number of latent variables in the model [29]. The PLSR was performed using R software version 4.0.2. Root mean square error (RMSE) and coefficient of determination R^2 were employed to evaluate the performances of the models. The model with higher values of R^2 and lower values of RMSE was deemed as the best model for soil salinity estimation.

Table 2. Soil salinity and vegetation indices derived from the Sentinel 2A multispectral satellite image.

Acronym	Spectral Index	Formula	Reference
SI1	Salinity Index 1	$\sqrt{BXR}$	[30]
SI2	Salinity Index 2	$\sqrt{GXR}$	[30]
SI3	Salinity Index 3	$\sqrt{(G^2 + R^2 + NIR^2)}$	[31]
SI4	Salinity Index 4	$\sqrt{(G^2 + R^2)}$	[31]
SI5	Salinity Index 5	B/R	[32]
SI6	Salinity Index 6	$(B - R)/(B + R)$	[32]
SI7	Salinity Index 7	$(GXR)/B$	[32]
SI8	Salinity Index 8	$(BXR)/G$	[32]
SI9	Salinity Index 9	$(RXNIR)/G$	[32]
S10RED	Salinity index 10 red-edge 3	$\sqrt{(G^2 + RedEdge^2 + NIR^2)}$	[16]
SI11	Salinity Index 11	$(BXRedEdge)/G$	[16]
SI12	Salinity Index 12	$(SWIR2 - G)/(G - SWIR1)$	[16]
NDSI	Normalized Differential Salinity Index	$(R - NIR)/(R + NIR)$	[33]
INN1	Intensity Index 1	$(G + R)/2$	[16]
INN2	Intensity Index 2	$(G + R + NIR)/2$	[16]

The common methods for soil salinity detection involve using direct soil reflectance (salinity indices) [18,20] either alone or along with vegetation reflectance (vegetation indices) in regions of thickly vegetated soils [34,35]. However, when vegetation is not present, the different levels of salt in the soils result in different levels of reflectance, and these differences in soil reflectance could be used in determining levels of salinity. In our case, there was no vegetation, since the soil samples were obtained during post-harvest and ploughing season. Therefore, we have only used soil salinity indices in salinity detection, which is a widely used technique [16,18,20,36].

2.5. Land Use Classification and Delineation of Paddy Land

The pre-processed Sentinel 2A satellite image was classified into six basic land use classes, including paddy land, other crops, built-up area, barren land, wet land and water bodies, using a supervised maximum likelihood classifier. In total, 2136 training sites were randomly collected according to the typical representative of land use classes from Google Earth Pro. An accuracy assessment of the classified map was performed from 992 randomly collected test samples from Google Earth and the field visits. The overall accuracy was 90.5% with a kappa value of 0.85. Built-up area land use was clipped from the study area boundary and the rest of the area was used for salinity mapping. Paddy land use was extracted and overlayed with the resulting salinity distribution map to estimate the extent of salinity on active paddy lands.

3. Results

3.1. Descriptive Statistics of the EC Data

The descriptive statistics of the whole dataset are presented in Table 3. For the whole dataset, the EC ranged from 0.05 to 34 dS m^{-1}. The mean and SD were 3.51 dS m^{-1} and 5.8 dS m^{-1}, respectively. The higher coefficient of variation of EC was 167.3, and this indicates that the soil is highly variable with respect to EC.

Table 3. Summary statistics of the whole set of EC data.

	Descriptive Statistics (dS m^{-1})
Range	0.05–34.1
Median	0.58
Mean	3.51
1st Qu	0.21
3rd Qu	4.39
SD	5.8
CV (%)	167.3

3.2. Relationship between EC and Spectral Reflectance Bands

Since the EC data of the soil samples were positively skewed, a log transformation was applied to conform them to normality. The correlation between the EC values of the soil samples, the band values and the spectral salinity indices derived from the Sentinel 2A satellite image is visualized in Figure 2. Elevation data extracted from the digital elevation model (DEM) were included as the only environmental covariate. The DEM (1 m resolution) was produced from spot heights and contour data obtained from the National Survey Department of Sri Lanka. The correlation coefficient results showed that the SI5 and SI6 indices exhibited positive moderate correlations with EC. SWIR2 showed moderate negative correlation, and SWIR1 and SI3 showed weak correlations. The correlation between spectral indices and EC performed better than that with spectral bands. However, none of the single bands or indices were capable of effective mapping with acceptable accuracy. Hence optimum combinations of bands and indices were used in the models.

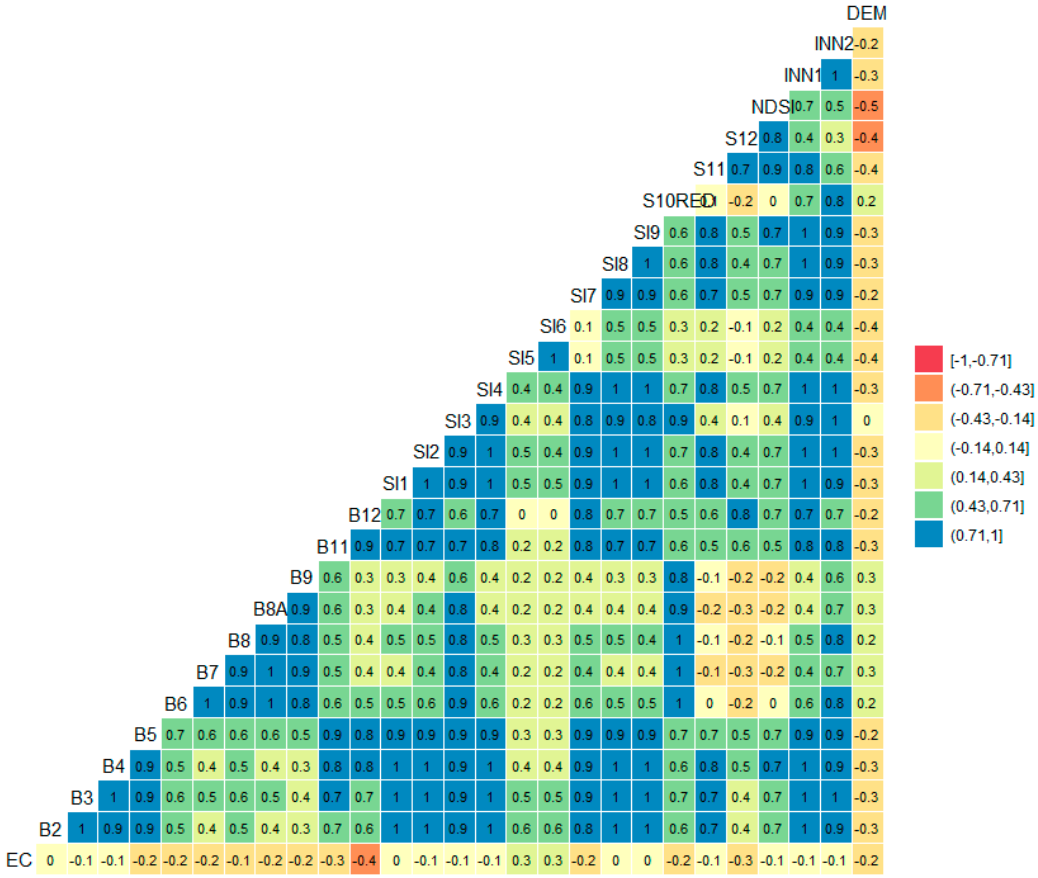

Figure 2. Correlation matrix of EC and individual bands of Sentinel 2A satellite imagery, and the spectral indices tested are shown.

Richards [9] categorized soil salinity into five classes according to the impact level on crops: non-saline (0–2 dS m^{-1}), slightly saline (2–4 dS m^{-1}), moderately saline (4–8 dS m^{-1}), highly saline (8–16 dS m^{-1}) and extremely saline (above 16 dS m^{-1}). However, rice crops are more sensitive to even a 3 dS m^{-1} salinity level for most cultivated varieties [37]. Figure 3 shows the relationship between the EC values of soil samples and the spectral reflectance of the Sentinel 2A satellite data. Except for extremely saline soil samples, others with different salinity levels show a very similar spectral reflectance trend. The spectral reflectance increases from blue to NIR (i.e., vegetation red edge), reaches a peak at SWIR1 and then decreases from SWIR1 to SWIR2. Extremely saline soil samples exhibit the lowest reflectance across all bands, which shows that the spectral reflectance of soil samples is inversely related to their salt content, which is in line with previous research [38–40].

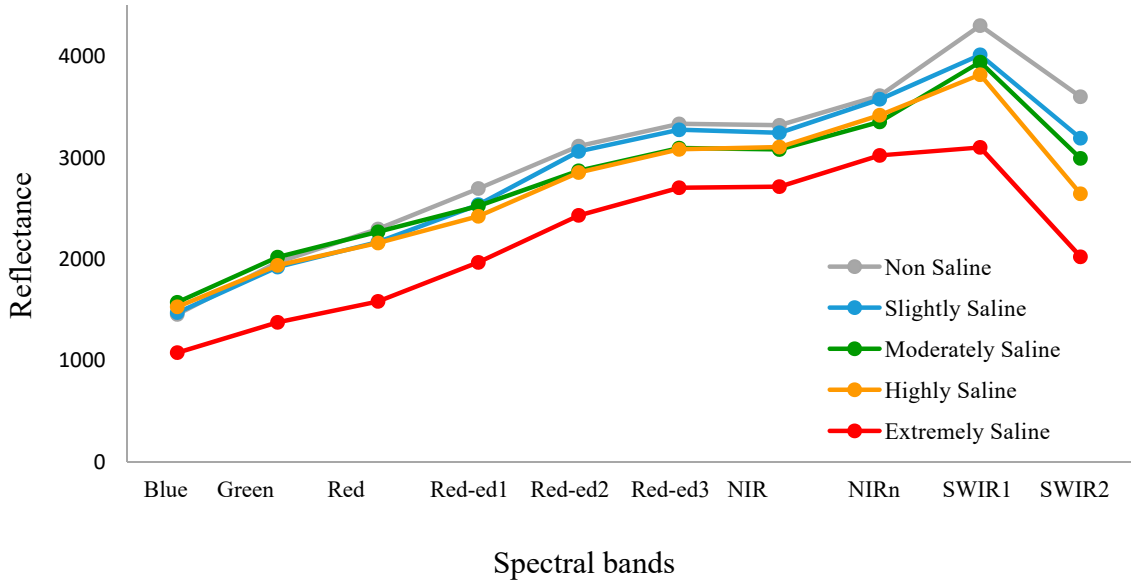

Figure 3. Sentinel 2A spectral reflectance spectrum of soil samples with different salinity levels.

3.3. Model Results

The best possible combination of variables from the Pearson correlation coefficient and VIP were used in the calibration of the models. The results indicate (Table 4) that PLSR-PCC recorded better results, with 0.69 R^2 and 0.4830 RMSE, compared to PLSR-VIP, where the R^2 and RMSE were 0.66 and 0.5072, respectively.

Table 4. PLSR model results.

	R^2	RMSE
PLSR-PCC	0.69	0.4830
PLSR-VIP	0.66	0.5072

* PLSR-PCC: PLSR model with variables chosen according to the Pearson correlation co-efficient
* PLSR-VIP: PLSR model with variables chosen according to the VIP.

The calibrated PLSR-PCC model was used to generate the soil salinity distribution map of Jaffna Peninsula (Figure 4). The soil salinity values were classified into five salinity classes as aforementioned. The spatial distribution of soil salinity map of Jaffna Peninsula shows that the saline soils are clustered all over the coastal lowlands of Jaffna Peninsula, covering approximately 401 ha (32.8%), particularly around the lagoonal areas. The majority of them are paddy lands. The areas with high salinity are located in the north-east, south-east and south-west parts of Jaffna mainland.

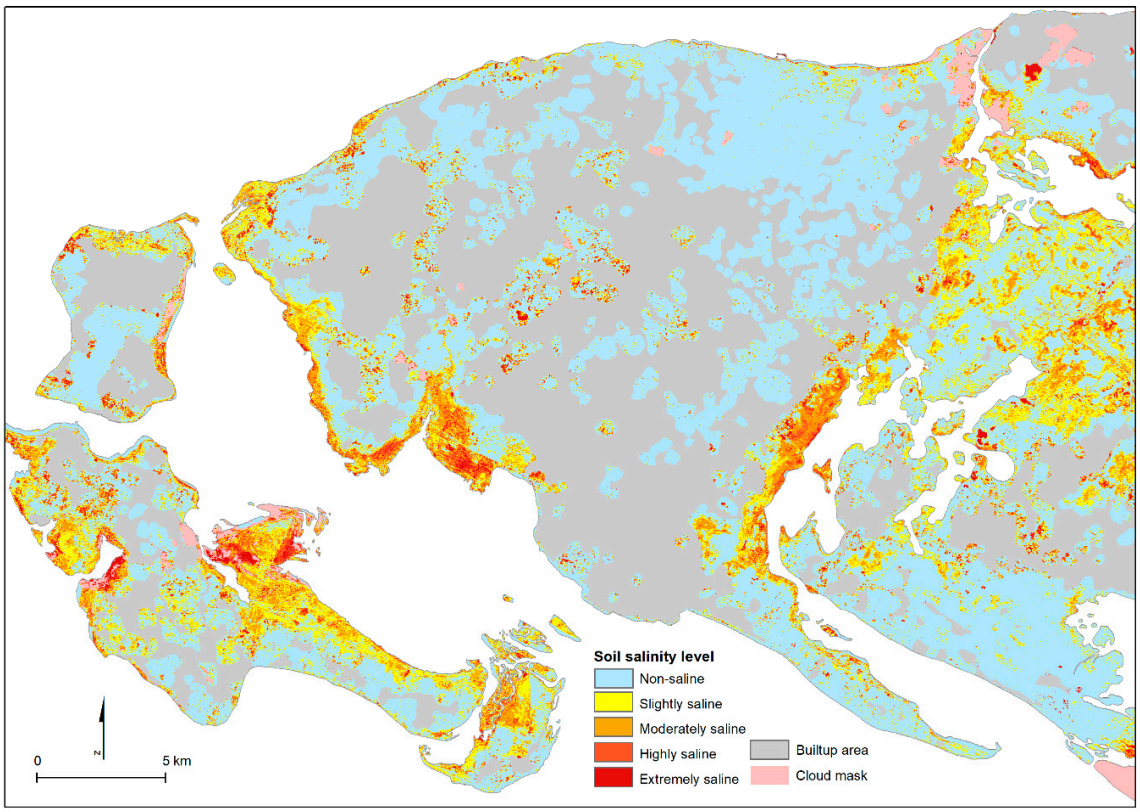

Figure 4. Soil salinity distribution map of Jaffna Peninsula as derived from the PLSR-PCC model.

3.4. Distribution of Soil Salinity in Paddy Lands

The spatial distribution of paddy lands affected by different salinity levels, obtained from an overlay analysis with the soil salinity map (Figure 5), indicated that the paddy cultivations in the lowland regions were greatly affected by salinity. The intensively salt-affected paddy lands were located in the north-eastern and western parts of the Jaffna mainland. About 46% of the total paddy land area of Jaffna Peninsula was affected by salt (Figure 6). Slightly saline paddy land soil accounted for 14.8% of the total paddy land area. Moderately saline and highly saline paddy land soil accounted for 9.2% and 8.6%, respectively, of all paddy lands. Importantly, 13% of paddy lands were extremely saline. Paddy cultivation in the islands was less affected by salinity, as compared to the mainland.

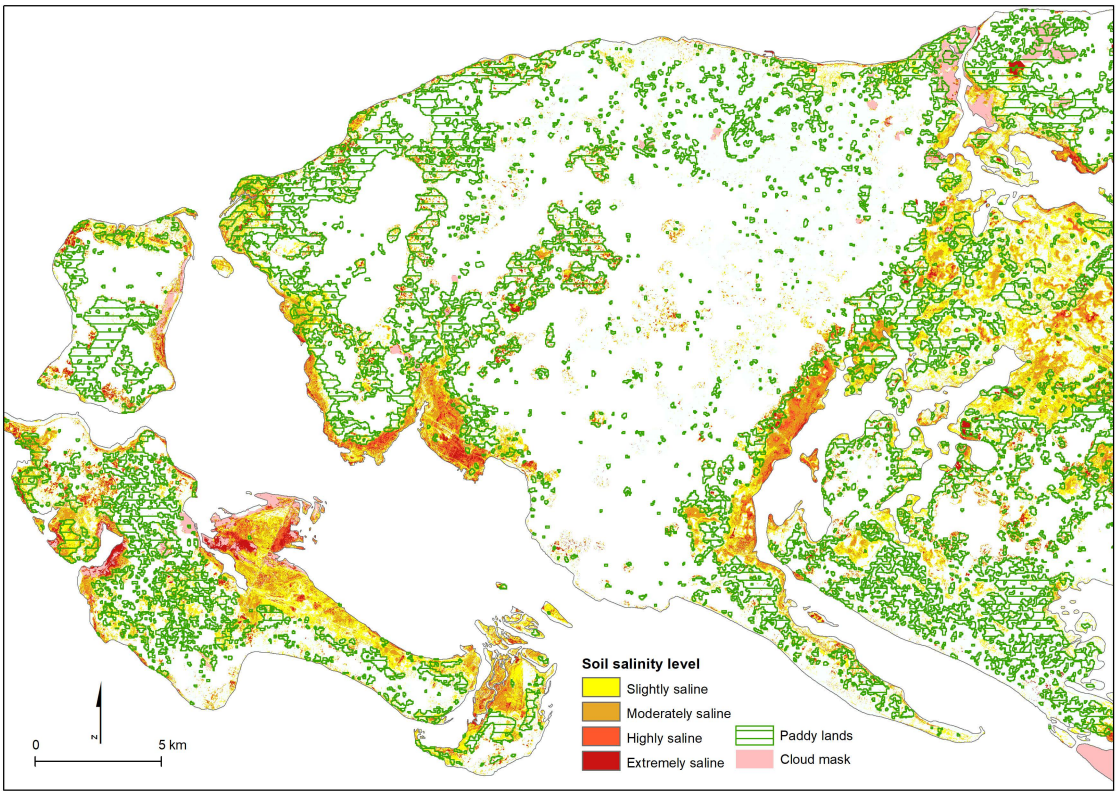

Figure 5. Spatial distribution of paddy land use and overlaid on soil salinity map of Jaffna Peninsula.

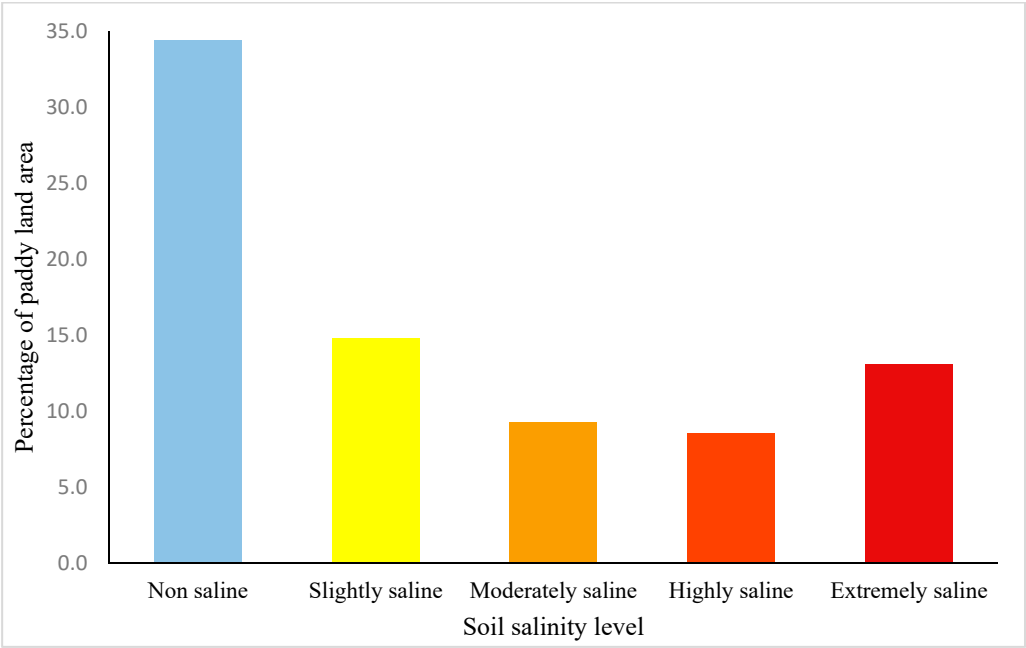

Figure 6. Percentage of paddy lands affected by various levels of soil salinity.

4. Discussion

Jaffna Peninsula is characterized as a semi- arid lowland region in Sri Lanka situated at a highly dynamic ocean–atmosphere interface, which makes the region more vulnerable to salinization. Jaffna Peninsula has been experiencing progressive seawater intrusion [41,42] into the coastal aquifers since the 1960s [43] due to climate change and its ever increasing demand for groundwater resources. In addition, tides and storms periodically bring brackish seawater from the ocean to lagoons and

nearby coastal lands. Furthermore, high evaporation rates during the drier seasons [28] and a lack of drainage in soil increase the accumulation of salt over time [38]. This situation is also exacerbated by heavy rainfall and drought occurring frequently due to climate change [44].

This study focused on developing a soil salinity map to investigate the extent and severity of soil salinization using Sentinel 2A satellite data. The results reveal that, contrary to similar studies, spectral bands of the Sentinel 2A satellite imagery and derived salinity indices showed relatively poor correlation with EC values, which could be due to the larger study area. The visible spectral bands showed no significant correlation with EC. SWIR bands showed the largest correlation values (0.30 and 0.44) among the spectral bands, followed by vegetation red edge bands. As expected, the terrain covariate DEM showed a significant relationship with EC, which aligned with research by Li, et al. [45]. Among the salinity indices, SI5, SI6 and SI12 had significant correlations with EC. The spectral reflectance trend of the Sentinel 2A satellite imagery with different salinity levels reveals that the highest salt content samples (extreme salinity) showed the lowest reflectance, and the lowest salinity had the highest reflectance. This finding is consistent with that of Nawar, Buddenbaum, Hill and Kozak [38], Li, Ren, Zhao and Liang [39], Abuelgasim and Ammad [40]. The relationship is more likely due to the soil moisture, surface roughness and organic carbon content [38,46]. Further, high-salinity soil samples with lower reflectance in the NIR were reported in the Mekong delta by Nguyen, Liou, Tran, Hoang and Nguyen [34], where the hot and dry climate of the study areas was attributed to the lower reflectance trend.

The findings indicate that the PLSR model yields a satisfactory relationship between the measured and predicted EC values, with an R^2 value of 0.69. In addition, according to Farifteh, et al. [47] models with an R^2 value above 0.66 can provide an acceptable approximate estimate, thus our results indicate that the spectral reflectance of Sentinel 2A satellite data has a great potential to yield a fairly accurate soil salinity map for Jaffna Peninsula. This finding aligns with the results of Wang, Ding, Yu, Ma, Zhang, Ge, Teng, Li, Liang, Lizaga, Chen, Yuan and Guo [16], who found that Sentinel 2A satellite data with a PLSR model provide greater prediction power for the assessment of soil salinity in semi-arid regions. Therefore, this study demonstrated that this model could satisfactorily map soil salinity over the large area of Jaffna Peninsula in Sri Lanka.

The intensity of soil salinity decreases significantly with increasing distance from the coast. Generally, higher elevation (i.e., >10 m) areas are less affected by salts. This shows that seawater intrusion and inundation could play a major role in the salinization of lands. More than 203 ha of land (16%) is affected by moderate to high salinization, and 4% of land is extremely saline. Increasing salinity levels in the groundwater of coastal Jaffna Peninsula over the past several decades have been widely reported, and salty groundwater may have primarily contributed to the soil salinization. In poor drainage conditions, when the groundwater table rises, the saline groundwater reaches the top soil layers [48]. This is in agreement with the previous studies of Gopalakrishnan, Kumar and Mikunthan [27] and Gunaalan, Ranagalage, Gunarathna, Kumari, Vithanage, Srivaratharasan, Saravanan and Warnasuriya [26], where the groundwater salinization in the dry seasons was reported in the north-east, south-east and south-west regions of Jaffna—areas where highly saline soils were distributed.

Rice is the staple food in Sri Lanka, and any salinity beyond the threshold level of 3 dS m^{-1} would cause reductions in yield by up to 12% [49,50]. Studies have shown that the crop is salt-sensitive due to its geomorphological location (lowland) and edaphic needs, such as silt clay [51–53]. The high-density saline soils that were established to be predominant in the lowland paddy field areas confirm that salinity is an explicit threat to rice cultivation in the area. Unlike other parts of Sri Lanka, rice is cultivated during only one season ("Maha") in Jaffna Peninsula due to a lack of irrigation water availability. In this context, having 46% of paddy lands affected by soil salinity is an alarming threat to the sustainability of paddy cultivation in Jaffna Peninsula. This agrees with our previous study [27] and field investigations in that the increasing salinization could be the cause of paddy land abandonment

in the south-east and south-west regions of Jaffna Peninsula. However, an investigation into long-term soil salinity changes is required to further validate this concept.

The increasing food demand of the growing population, and the pressure thus exerted on the already vulnerable fertile agricultural lands, are issues of concern worldwide. The total Jaffna Peninsula is surrounded by water on three sides, and no part is more than 10 km from the coast. In our previous study, we reported that the majority of the population (58.3%) in Jaffna Peninsula are living close to the coast (within 2 km of the coastline) in high-density settlements [54]. Further, 62% of the population are located within 5 masl, and are less than 3 km from the coast. In addition, we have also found that a number of human resettlements established after the civil war were in areas very close to the coast. This increasing population along the coastal fringes of Jaffna Peninsula will further increase the vulnerability of the paddy lands in the coastal lowlands to salinization [55]. The subsequent construction of more new wells and the over-extraction of groundwater is likely to increase seawater intrusion into coastal aquifers [27].

The accuracy of the model's ability to estimate soil salinity is limited by other soil properties, such as soil moisture, soil clay content, soil organic content and vegetation [56]. We observed during the soil sample collection period that most of the paddy lands were ploughed with organic matter, which could have influenced the actual salt content prediction of the soil [34]. Further, another limitation of soil mapping also comes with the uncertainty of the relationship between the salt content of the soil and remote sensing data. For instance, although atmospheric and radiometric corrections were performed, and soil samples that fell within the cloud cover areas were removed, the potential shadows and terrain factors may cause errors.

Semi-arid coastal regions are particularly vulnerable to a range of natural and climate change-induced hazards, such as tidal surges, rising sea levels, coastal erosion and seawater intrusion. It is estimated that by 2050, across all four Intergovernmental Panel on Climate Change Representative Concentration Pathways (IPCC RCP) scenarios, about 6.8–13% of the lands of Jaffna Peninsula will be subjected to inundation [57]. At the same time, increases in population will accelerate the demand for lands and water resources. In this context, the findings of this study have identified areas at risk of salinization where immediate attention is required to prevent further land degradation. Additionally, the maps created showing the vulnerability of paddy lands to salinity show that mitigation and adaptation efforts are necessary to reclaim the impacted paddy lands so as to ensure the sustainability of rice production and food security in Jaffna Peninsula.

Jaffna Peninsula has been ravaged by war over the last 40 years. Field work in remote sensing is still fraught with danger, as there are still many unexploded ordinances present. In such a situation, a remote sensing-derived product will be extremely useful for the mapping and monitoring of soil salinity. This study has shown that Sentinel 2 satellite data have the capability to map soil salinity with reasonable accuracy, and thus provide a viable option for soil salinity mapping and monitoring.

The correct use of soil, one of the non-renewable resources involved in human activities, affects the long-term sustainability of agricultural systems. Nevertheless, soil conservation and protection is paramount to reaching the UN Sustainable Development Goals (SDG) 2: Zero hunger, SDG 3: Good health and wellbeing, SDG 6: Clean water and sanitation, SDG 13: Climate action, and SDG 15: Life on land. Therefore, we believe that the results from this study will be useful for the implementation of policies and regulations to improve food production and societal environmental sustainability regarding the soil.

5. Conclusions

Soil salinity distribution in the Jaffna Peninsula was mapped using Sentinel 2A satellite imagery, utilizing the various spectral bands and salinity indices. Satisfactory results were achieved based on the PLSR model (R^2 = 0.69). The PLSR model was then applied to the reflectance values of each pixel of the Sentinel 2A satellite image to map soil salinity for the entire study area. The results revealed that 32.8% of the study area is affected by salinity. Highly saline lands are distributed along the coastal

lowlands and areas around the lagoons. Approximately 45% of the paddy lands are salt-affected, and among them, 13% of paddy lands were extremely saline. Particularly highly intensive saline soils were located in the north-eastern and western paddy lands of Jaffna mainland. This study demonstrates that Sentinel images offer salinity estimations for the topsoil with an acceptable accuracy in semi-arid regions. Future research will focus on assessing the long-term salinity changes that accompany land cover change in order to confirm the impact of salinity on coastal agricultural lands, and determine the sustainability of paddy cultivation in Jaffna Peninsula under the impacts of climate change.

Author Contributions: Conceptualization: T.G. and L.K.; methodology: T.G. and L.K.; formal analysis; T.G.; data curation, T.G. and L.K.; writing—original draft preparation: T.G.; writing—review and editing, L.K.; supervision, L.K. Both authors have read and agreed to the published version of the manuscript. All authors have read and agreed to the published version of the manuscript.

Funding: This research received no external funding.

Conflicts of Interest: The authors declare no conflict of interest.

References

1. Eswaran, H.; Lal, R.; Reich, P. Land degradation: An overview. Available online: https://www.nrcs.usda.gov/wps/portal/nrcs/detail/soils/use/?cid=nrcs142p2_054028 (accessed on 8 October 2020).
2. Olsson, L.; Barbosa, H.; Bhadwal, S.; Cowie, A.; Delusca, K.; Flores-Renteria, D.; Hermans, K.; Jobbagy, E.; Kurz, W.; Li, D. Land Degradation: IPCC Special Report on Climate Change, Desertification, Land Degradation, Sustainable Land Management, Food Security, and Greenhouse Gas Fluxes in Terrestrial Ecosystems. In *IPCC Special Report on Climate Change, Desertification, Land 5 Degradation, Sustainable Land Management, Food Security, and 6 Greenhouse gas fluxes in Terrestrial Ecosystems*; Intergovernmental Panel on Climate Change (IPCC): Geneva, Switzerland, 2019; p. 112.
3. Schutter, O.D. Towards a Common Food Policy for the European Union. 2019. Available online: http://www.ipes-food.org/_img/upload/files/CFP_FullReport.pdf (accessed on 8 October 2020).
4. Veerman, C.; Correia, T.P.; Bastioli, C.; Biro, B.; Bouma, J.; Cienciala, E.; Emmett, B.; Frison, E.A.; Grand, A.; Filchev, L.H.; et al. *Caring for Soil is Caring for Life—Ensure 75% of Soils are Healthy by 2030 for Healthy Food, People, Nature and Climate*; European Commission: Luxembourg, 2020.
5. Rengasamy, P. Soil Salinization. *Oxford Bibliogr.* **2014**. [CrossRef]
6. Imadi, S.R.; Shah, S.W.; Kazi, A.G.; Azooz, M.M.; Ahmad, P. Chapter 18—Phytoremediation of Saline Soils for Sustainable Agricultural Productivity. In *Plant Metal Interaction*; Ahmad, P., Ed.; Elsevier: Amsterdam, The Netherlands, 2016; pp. 455–468.
7. Jamil, A.; Riaz, S.; Ashraf, M.; Foolad, M.R. Gene Expression Profiling of Plants under Salt Stress. *Crit. Rev. Plant Sci.* **2011**, *30*, 435–458. [CrossRef]
8. Shrivastava, P.; Kumar, R. Soil salinity: A serious environmental issue and plant growth promoting bacteria as one of the tools for its alleviation. *Saudi J. Biol. Sci.* **2015**, *22*, 123–131. [CrossRef]
9. Richards, L.A. Diagnosis and Improvement of Saline and Alkali Soils. *Soil Sci.* **1954**, *78*, 154. [CrossRef]
10. Allbed, A.; Kumar, L. Soil Salinity Mapping and Monitoring in Arid and Semi-Arid Regions Using Remote Sensing Technology: A Review. *Adv. Remote Sens.* **2013**, *2*, 373–385. [CrossRef]
11. Nouri, H.; Borujeni, S.C.; Alaghmand, S.; Anderson, S.J.; Sutton, P.C.; Parvazian, S.; Beecham, S. Soil Salinity Mapping of Urban Greenery Using Remote Sensing and Proximal Sensing Techniques; The Case of Veale Gardens within the Adelaide Parklands. *Sustainability* **2018**, *10*, 2826. [CrossRef]
12. Allbed, A.; Kumar, L.; Aldakheel, Y.Y. Assessing soil salinity using soil salinity and vegetation indices derived from IKONOS high-spatial resolution imageries: Applications in a date palm dominated region. *Geoderma* **2014**, *230*, 1–8. [CrossRef]
13. Bannari, A.; El-Battay, A.; Bannari, R.; Rhinane, H. Sentinel-MSI VNIR and SWIR Bands Sensitivity Analysis for Soil Salinity Discrimination in an Arid Landscape. *Remote Sens.* **2018**, *10*, 855. [CrossRef]
14. Morgan, R.; El-Hady, M.A.; Rahim, I. Soil salinity mapping utilizing sentinel-2 and neural networks. *Indian J. Agric. Res.* **2018**, *52*, 524–529.
15. Farahmand, N.; Sadeghi, V. Estimating Soil Salinity in the Dried Lake Bed of Urmia Lake Using Optical Sentinel-2 Images and Nonlinear Regression Models. *J. Indian Soc. Remote Sens.* **2020**, *48*, 675–687. [CrossRef]

16. Wang, J.; Ding, J.; Yu, D.; Ma, X.; Zhang, Z.; Ge, X.; Teng, D.; Li, X.; Liang, J.; Lizaga, I.; et al. Capability of Sentinel-2 MSI data for monitoring and mapping of soil salinity in dry and wet seasons in the Ebinur Lake region, Xinjiang, China. *Geoderma* **2019**, *353*, 172–187. [CrossRef]
17. Davis, E.; Wang, C.; Dow, K. Comparing Sentinel-2 MSI and Landsat 8 OLI in soil salinity detection: A case study of agricultural lands in coastal North Carolina. *Int. J. Remote Sens.* **2019**, *40*, 6134–6153. [CrossRef]
18. Wang, J.; Ding, J.; Yu, D.; Teng, D.; He, B.; Chen, X.; Ge, X.; Zhang, Z.; Wang, J.; Yang, X.; et al. Machine learning-based detection of soil salinity in an arid desert region, Northwest China: A comparison between Landsat-8 OLI and Sentinel-2 MSI. *Sci. Total Environ.* **2020**, *707*, 136092. [CrossRef] [PubMed]
19. Taghadosi, M.M.; Hasanlou, M.; Eftekhari, K. Retrieval of soil salinity from Sentinel-2 multispectral imagery. *Eur. J. Remote Sens.* **2019**, *52*, 138–154. [CrossRef]
20. Gorji, T.; Yildirim, A.; Hamzehpour, N.; Tanik, A.; Sertel, E. Soil salinity analysis of Urmia Lake Basin using Landsat-8 OLI and Sentinel-2A based spectral indices and electrical conductivity measurements. *Ecol. Indic.* **2020**, *112*, 106173. [CrossRef]
21. Perera, M.; Ranasinghe, T.; Piyadasa, R.; Jayasinghe, G. Risk of seawater intrusion on coastal community of Bentota river basin Sri Lanka. *Procedia Eng.* **2018**, *212*, 699–706. [CrossRef]
22. NWDB. *Environmental Impact Assessment: Sri Lanka: Jaffna and Kilinochchi Water Supply Project, Additional Financing—Seawater Desalination Plant and Potable Water Conveyance System*; National Water Supply and Drainage Board (NWDB) & Government of Sri Lanka (GoSL): Ratmalana, Sri Lanka, 2017.
23. Wijeyaratne, W.M.D.N.; Subanky, S. Assessment of the Efficacy of Home Remedial Methods to Improve Drinking Water Quality in Two Major Aquifer Systems in Jaffna Peninsula, Sri Lanka. *Science* **2017**, *2017*, 1–6. [CrossRef]
24. Gunaalan, K.; Manjula, R.; Vithanage, M. *Assessing the Extent of Saltwater Intrusion at Vadamaradchchi Lagoon: In Jaffna Peninsula in Sri Lanka using GIS Techniques*; LAP LAMBERT Academic Publishing: Saarbrücken, Germany, 2015.
25. Sivakumar, S. Reclamation of Land and Improve Water Productivity of Jaffna Peninsula of Northern Sri Lanka by Improving the Water Quality of the Lagoons. *Int. Res. J. Sci. IT Manag.* **2013**, *2*, 20–27.
26. Gunaalan, K.; Ranagalage, M.; Gunarathna, M.; Kumari, M.; Vithanage, M.; Srivaratharasan, T.; Saravanan, S.; Warnasuriya, T.W.S. Application of Geospatial Techniques for Groundwater Quality and Availability Assessment: A Case Study in Jaffna Peninsula, Sri Lanka. *ISPRS Int. J. Geo Inf.* **2018**, *7*, 20. [CrossRef]
27. Gopalakrishnan, T.; Kumar, L.; Mikunthan, T. Assessment of Spatial and Temporal Trend of Groundwater Salinity in Jaffna Peninsula and Its Link to Paddy Land Abandonment. *Sustainability* **2020**, *12*, 3681. [CrossRef]
28. Mikunthan, T.; Vithanage, M.; Pathmarajah, S.; Arasalingam, S.; Ariyaratne, R.; Manthrithilake, H. Hydrogeochemical characterization of Jaffna's aquifer systems in Sri Lanka. In *Hydrogeochemical Characterization of Jaffna's Aquifer Systems in Sri Lanka*; International Water Management Institute (IWMI): Colombo, Sri Lanka, 2013; p. 69.
29. Rossel, R.A.V. Robust Modelling of Soil Diffuse Reflectance Spectra by "Bagging-Partial Least Squares Regression". *J. Near Infrared Spectrosc.* **2007**, *15*, 39–47. [CrossRef]
30. Khan, N.M.; Rastoskuev, V.V.; Sato, Y.; Shiozawa, S. Assessment of hydrosaline land degradation by using a simple approach of remote sensing indicators. *Agric. Water Manag.* **2005**, *77*, 96–109. [CrossRef]
31. Douaoui, A.E.K.; Nicolas, H.; Walter, C. Detecting salinity hazards within a semiarid context by means of combining soil and remote-sensing data. *Geoderma* **2006**, *134*, 217–230. [CrossRef]
32. Khan, S.; Abbas, A. Using remote sensing techniques for appraisal of irrigated soil salinity. In Proceedings of the International Congress on Modelling and Simulation, Christchurch, New Zealand, 10–12 December 2007; pp. 2632–2638.
33. Major, D.J.; Baret, F.; Guyot, G. A ratio vegetation index adjusted for soil brightness. *Int. J. Remote Sens.* **1990**, *11*, 727–740. [CrossRef]
34. Nguyen, K.-A.; Liou, Y.-A.; Tran, H.-P.; Hoang, P.-P.; Nguyen, T.-H. Soil salinity assessment by using near-infrared channel and Vegetation Soil Salinity Index derived from Landsat 8 OLI data: A case study in the Tra Vinh Province, Mekong Delta, Vietnam. *Prog. Earth Planet. Sci.* **2020**, *7*, 1–16. [CrossRef]
35. Gorji, T.; Tanik, A.; Sertel, E. Soil Salinity Prediction, Monitoring and Mapping Using Modern Technologies. *Procedia Earth Planet. Sci.* **2015**, *15*, 507–512. [CrossRef]

36. Abbas, A.; Khan, S.; Hussain, N.; Hanjra, M.A.; Akbar, S. Characterizing soil salinity in irrigated agriculture using a remote sensing approach. *Phys. Chem. Earth Parts A/B/C* **2013**, *55*, 43–52. [CrossRef]
37. Hoang, T.M.L.; Tran, T.N.; Nguyen, T.K.T.; Williams, B.; Wurm, P.; Bellairs, S.; Mundree, S.G. Improvement of Salinity Stress Tolerance in Rice: Challenges and Opportunities. *Agronomy* **2016**, *6*, 54. [CrossRef]
38. Nawar, S.; Buddenbaum, H.; Hill, J.; Kozak, J. Modeling and Mapping of Soil Salinity with Reflectance Spectroscopy and Landsat Data Using Two Quantitative Methods (PLSR and MARS). *Remote Sens.* **2014**, *6*, 10813–10834. [CrossRef]
39. Li, X.; Ren, J.; Zhao, K.; Liang, Z. Correlation between Spectral Characteristics and Physicochemical Parameters of Soda-Saline Soils in Different States. *Remote Sens.* **2019**, *11*, 388. [CrossRef]
40. Abuelgasim, A.; Ammad, R. Mapping soil salinity in arid and semi-arid regions using Landsat 8 OLI satellite data. *Remote Sens. Appl. Soc. Environ.* **2019**, *13*, 415–425. [CrossRef]
41. Chandrajith, R.; Diyabalanage, S.; Premathilake, K.; Hanke, C.; Van Geldern, R.; Barth, J.A.C. Controls of evaporative irrigation return flows in comparison to seawater intrusion in coastal karstic aquifers in northern Sri Lanka: Evidence from solutes and stable isotopes. *Sci. Total Environ.* **2016**, *548*, 421–428. [CrossRef] [PubMed]
42. Edirisinghe, E.; Karunarathne, G.; Tilakarathna, I.; Gunasekara, J.; Priyadarshanee, K. Isotope and chemical assessment of natural water in the Jaffna Peninsula in northern Sri Lanka for groundwater development aspects. *Isot. Environ. Health Stud.* **2020**, *56*, 205–219. [CrossRef] [PubMed]
43. Rajasooriyar, L.; Mathavan, V.; Dharmagunawardhane, A.H.; Nandakumar, V. Groundwater quality in the Valigamam region of the Jaffna Peninsula, Sri Lanka. *Geol. Soc. Lond. Spéc. Publ.* **2002**, *193*, 181–197. [CrossRef]
44. Chhogyel, N.; Kumar, L.; Bajgai, Y. Consequences of Climate Change Impacts and Incidences of Extreme Weather Events in Relation to Crop Production in Bhutan. *Sustainability* **2020**, *12*, 4319. [CrossRef]
45. Li, Z.; Li, Y.; Xing, A.; Zhuo, Z.; Zhang, S.; Zhang, Y.; Huang, Y. Spatial Prediction of Soil Salinity in a Semiarid Oasis: Environmental Sensitive Variable Selection and Model Comparison. *Chin. Geogr. Sci.* **2019**, *29*, 784–797. [CrossRef]
46. Bai, L.; Wang, C.; Zang, S.; Wu, C.; Luo, J.; Wu, Y. Mapping Soil Alkalinity and Salinity in Northern Songnen Plain, China with the HJ-1 Hyperspectral Imager Data and Partial Least Squares Regression. *Sensors* **2018**, *18*, 3855. [CrossRef]
47. Farifteh, J.; Van Der Meer, F.; Atzberger, C.; Carranza, E.J.M. Quantitative analysis of salt-affected soil reflectance spectra: A comparison of two adaptive methods (PLSR and ANN). *Remote Sens. Environ.* **2007**, *110*, 59–78. [CrossRef]
48. Brouwer, C.; Goffeau, A.; Heibloem, M. *Irrigation Water Management: Training Manual No. 1-Introduction to Irrigation*; Food and Agriculture Organization of the United Nations: Rome, Italy, 1985; pp. 102–103.
49. Wallender, W.W.; Tanji, K.K. *Agricultural Salinity Assessment and Management*; American Society of Civil Engineers (ASCE): Reston, VA, USA, 2011.
50. Grattan, S.R.; Zeng, L.; Shannon, M.C.; Roberts, S.R. Rice is more sensitive to salinity than previously thought. *Calif. Agric.* **2002**, *56*, 189–198. [CrossRef]
51. Thiam, S.; Villamor, G.B.; Kyei-Baffour, N.; Matty, F. Soil salinity assessment and coping strategies in the coastal agricultural landscape in Djilor district, Senegal. *Land Use Policy* **2019**, *88*, 104191. [CrossRef]
52. Barbiero, L.; Cunnac, S.; Mané, L.; Laperrousaz, C.; Hammecker, C.; Emaeght, J.-L. Salt distribution in the Senegal middle valley. *Agric. Water Manag.* **2001**, *46*, 201–213. [CrossRef]
53. Nhan, D.K.; Phap, V.A.; Phuc, T.H.; Trung, N.H. Rice production response and technological measures to adapt to salinity intrusion in the coastal Mekong delta. 2012. Available online: http://www.mpowernetwork.org/Knowledge_Bank/Key_Reports/PDF/Research_Reports/Rice_response_to_salinity.pdf?tabid=34059 (accessed on 8 October 2020).
54. Gopalakrishnan, T.; Kumar, L.; Hasan, K. Coastal settlement patterns and exposure to sea-level rise in the Jaffna Peninsula, Sri Lanka. *Popul. Environ.* **2020**, *42*, 1–17. [CrossRef]
55. Gopalakrishnan, T.; Hasan, K.; Haque, A.T.M.S.; Jayasinghe, S.L.; Kumar, L. Sustainability of Coastal Agriculture under Climate Change. *Sustainability* **2019**, *11*, 7200. [CrossRef]

56. Peng, J.; Ji, W.; Ma, Z.; Li, S.; Chen, S.; Zhou, L.-Q.; Shi, Z. Predicting total dissolved salts and soluble ion concentrations in agricultural soils using portable visible near-infrared and mid-infrared spectrometers. *Biosyst. Eng.* **2016**, *152*, 94–103. [CrossRef]
57. Gopalakrishnan, T.; Kumar, L. Potential Impacts of Sea-Level Rise upon the Jaffna Peninsula, Sri Lanka: How Climate Change Can Adversely Affect the Coastal Zone. *J. Coast. Res.* **2020**, *36*, 951–960. [CrossRef]